PD Diagnosis on 22.9kV XLPE Underground Cable using Ultra-wideband Sensor

Kyaw-Soe Lwin*, Kwang-Jin Lim*, Noh-Joon Park* and Dae-Hee Park†

Abstract – This paper presents compact low frequency ultra-wide band (UWB) sensor design and study of the partial discharge diagnosis by sensing electromagnetic pulse emitted from the partial discharge source with the newly designed UWB sensor. In this study, we designed a new type of compact low frequency UWB sensor based on microstrip antenna technology to detect both the low frequency and high frequency band of the partial discharge signal. Experiments of offline PD testing on medium voltage (22.9kV) underground cable mention the comparative results with the traditional HFCT as a reference sensor in the laboratory. In the series of comparative tests, the calibration signal injection test provided with the conventional IEC 60270 method and high voltage injection testing are included.

Keywords: 22.9kV XLPE cable, Off-line testing, Partial discharge, UWB sensor

1. Introduction

Partial discharges are localized electrical discharges that only partially bridge the insulation between conductors. Partial discharge is an important contributor to insulation deterioration. Failure of a high voltage cable can cause service interruption, costly location repairs, and loss of revenue. Utility experience shows that poor termination and jointing is a major source of cable failure. From the middle of the 20th century, people began researching on partial discharge. Partial discharge measurement is a well established criterion for the condition assessment and quality control of the high voltage electrical insulation. PD, originated from a micro-defect, incepts periodically according to the ac cycle of operating voltage and gradually degrades and erodes the polymeric material, eventually leading to breakdown [1].

During the partial discharge process, there are many forms of exchanges of energy such as electrical pulse current, dielectric loss, electromagnetic radiation, sound, ultrasonics, acoustics emission, increased gas pressured, and chemical reactions. In the detection of partial discharge, depending on the sensing of the kinds of energy exchange, different detecting methods were approached. In these methods, electromagnetic sensing is one of the best types of partial discharge detection and localization of PD source.

† Corresponding Author: Department of Electrical, Electronic & Information Eng., Wonkwang University, 344-2 Shinyoung-dong, Iksan, 570-749, Korea. (parkdh@wonkwang.ac.kr)
* Department of Electrical, Electronic & Information Eng., Wonkwang University
Received 22 January, 2008 ; Accepted 6 May, 2008

The occurrence of partial discharges in electrical insulation is always associated with the emission of electromagnetic pulses. A typical PD pulse has a rise time less than 1ns and a pulse width of several ns, implying a frequency domain of several GHz [2]. The electromagnetic emission propagates in all directions from the PD source.

Attenuation of electromagnetic PD pulse is a function of frequency along the propagation path. The higher the frequency, components will be attenuated rapidly when they travel along the cable [3, 4]. Therefore, the detectable electromagnetic (EM) wave emitted from the PD includes a broadband signal of VHF/UHF (Very High Frequency: 30MHz to 300MHz/ Ultra High frequency: 300MHz to 3000MHz) [5].

We tried to collect ultra-wide band (UWB) signals by using a new design compact low frequency UWB antenna sensor that can detect both low frequency and high frequency bands. This compact UWB antenna sensor is a modification of the conventional rectangular patch antenna by adding notches based on the microstrip line antenna theory. CST MS version 5.0 microwave simulation software is used to design and implement the UWB antenna sensor.

Off-line PD testing is deployed to examine the new UWB sensor to be comparative with the commercial high frequency current transformer (HFCT) in a laboratory. Some experimental results will be discussed over the HFCT sensor and our UWB antenna sensor in the detection of partial discharge in 22.9kV XLPE cable.

2. Sensor Design and Fabrication

2.1. Theory Background

Also called 'patch' antennas, microstrip patch antennas consist of a metallic patch that is on the top of a grounded dielectric substrate of thickness h, with relative permittivity ε_r and permeability μ_r *(usually taken 1)* as indicated in Fig. 1.

Patch antennas are widely used in microwave frequency range but they are often used in millimeter-wave frequency range as well by modifying various shapes of patch design [6]. The metallic patch essentially creates a resonant cavity, where the patch is the top of the cavity, the ground plane is the bottom of the cavity, and the edges of the patch form the sides of the cavity.

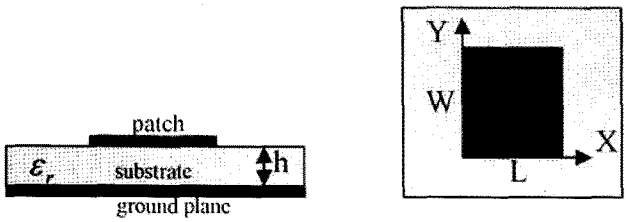

Fig. 1. Schematic diagram of patch antenna

The edges of the patch act approximately as an open-circuit boundary condition.

Hence, the patch cavity modes are described by a double index *(m,n)*. For *(m,n)* cavity mode of the rectangular patch, the electric field has the form

$$E_x(x,y) = A_{mn}\cos\left(\frac{m\pi x}{L}\right)\cos\left(\frac{n\pi x}{W}\right) \tag{1}$$

where L is the patch length and W is the patch width. The patch is usually operated in the *(1,0)* mode, so that L is the resonant dimension and the field is essentially constant in the y direction. The resonant frequency of the *(1,0)* mode is given by

$$f_0 = \frac{c}{2L_e\sqrt{\varepsilon_r}} \tag{2}$$

where c is the speed of light in a vacuum. To account for the fringing of the cavity fields at the edge of the patch, the length, the effective length L_e is chosen as

$$L_e = L + 2\Delta L \tag{3}$$

The Hammerstad formula for the fringing extension is [7] as follows.

$$\Delta L/h = 0.412\frac{(\varepsilon_{eff}+0.3)(\frac{W}{h}+0.264)}{(\varepsilon_{eff}-0.258)(\frac{W}{h}+0.8)}, \tag{4}$$

$$\varepsilon_{eff} = \frac{\varepsilon_r+1}{2} + \frac{\varepsilon_r-1}{2}(1+10\frac{h}{W})^{-1/2}. \tag{5}$$

For this mode the patch may be regarded as a wide microstrip line of width W, having resonant length L, which is approximately one half-wavelength in the dielectric. The current is maximum at the center of the patch, while the electric field is maximum at the "radiating" edges, x=0 and x=L. The width W is usually chosen to be larger than the length (W=1.5L is typical) to maximize the bandwidth, since the bandwidth is proportional to the width of the antenna bandwidth.

2.2 Sensor Design

The basis of this design is a rectangular element improved for wider bandwidth in low frequency and can detect signals from nearby fields. The width of the patch element is chosen 1.5 times of resonant length and modified with two notched patches which can be operated at both low and high frequencies of ultra-wide band operation. Our UWB sensor design was realized on FR4 substrate (ε_r =4.6, thickness=1.6mm) in order to keep costs down. At low frequencies the antenna size is the principal constraint, e.g. at 500MHz, the dimension of $\lambda/2$ antenna is 30 cm. It is very difficult to integrate as a sensor. Therefore it is necessary to reduce the antenna size at low frequency by using the notched patch antenna.

Simulation has been carried out with CST MWS version 5.0, to determine resonant bandwidth, return loss, and input impedance. The rectangular patch element is fed by microstrip line access, which is a common microwave transmission line that offers fairly good performances in the term of bandwidth at low cost.

To increase the antenna bandwidth, two cutting notches are used in the rectangular patch by controlling impedance stability [8]. These notches alter the electromagnetic coupling between the rectangular patch and ground plane. The width of the notches is particularly effective either at low or high frequencies. Matching improvement can be obtained by inserting a slot in the ground plane [9]. The characteristics of the antenna highly depend on the ground plane shape: The best result can be obtained changing ground length L_g with the ground slot of W_s.

These notches alter the electromagnetic coupling between the rectangular patch and ground plane [10]. In sensor design structure, the main rectangular patch element is modified with three notched patched elements and the

microstrip line feeding method is used. Some parts of the ground region are removed and modified with ground slots to obtain wider bandwidth.

2.3 Parameter Optimization and Simulation Results

The width of the notches is particularly effective either at low or high frequencies. Matching improvement can be obtained by inserting a slot in the ground plane [10]. The optimization parameters are W_{n1}, W_{n2}, W_f, and W_s while the feed line length is fixed L_f.

Several parameter optimizations are made by simulation to get the desired bandwidth and target frequency. An example of ground length optimization is given in Fig. 2.

The overall size of this structure is 110×64 mm^2. The width and the length of the feed line W_f and L_f are fixed at 1.6mm and 34.1mm to obtain the input impedance of 50Ω. The complete UWB antenna sensor design diagram is as shown in Fig. 3.

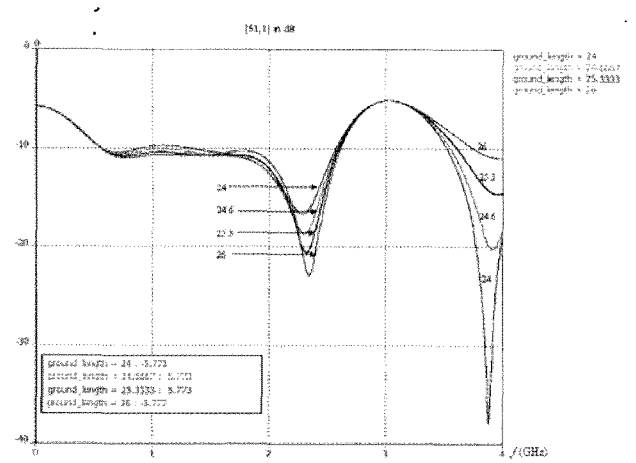

Fig. 2. Ground length optimization of S_{11} Vs frequency for 24 *mm*, 24.6 *mm*, 25.3 *mm* and 26 *mm*

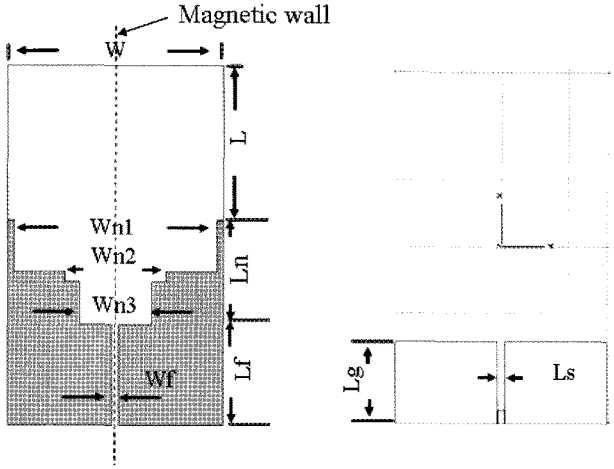

Fig. 3. The shape of the UWB sensor with microstrip line feed

After several simulations on the optimization of return loss with the desired frequencies, the final dimensions of the parameters in UWB sensors are given in Table. 1.

To decide the resonant frequency band of the sensor the return loss parameter S_{11} is carried out by simulation. The final simulation result of return loss with the optimized parameters is shown in Fig. 4.

The operating -10 dB bandwidth of the UWB sensor is from 365MHz to 2.624 GHz as presented in Fig. 4. It can also operate at -7dB of return loss at low frequency.

Table 1. The caption must be shown before the table.

Symbol	Dimension (mm)
W	64
L	47.5
W_{n1}	59
W_{n2}	29.5
W_{n3}	16
W_{nf}	1.6
L_n	28.4
L_f	34.5
L_{grd}	24.5
Ws	3

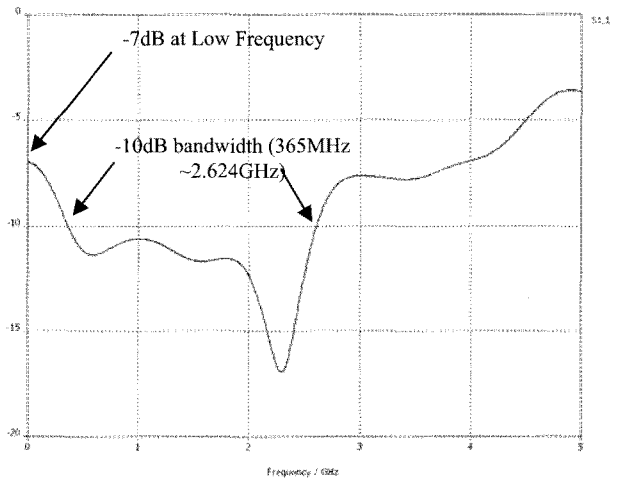

Fig. 4. Return loss simulation results with final dimensions showing -10dB bandwidth

The radiation pattern is one of the important characteristics of the antenna sensor. According to this radiation pattern, the location of the sensor is decided considering which place can be dedicated from the diagnosis object to achieve the better sensitivity.

The radiation pattern of this UWB sensor is measured in the simulation and is revealed in Fig. 5. According to Fig. 5 (a), (b), and (e), the maximum antenna gain at the main lobe is 7.26 dBi. (c) and (d) show the balance condition of left and right polarization with the gain of 4.25 dBi. This antenna sensor exhibits as a monopole directional antenna. Therefore, it can easily point the direction of the electromagnetic pulses coming from the PD source.

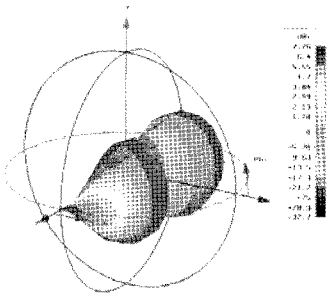

(a) Theta pattern of far-field radiation

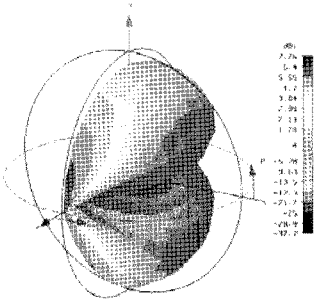

(b) Phi pattern of far field radiation

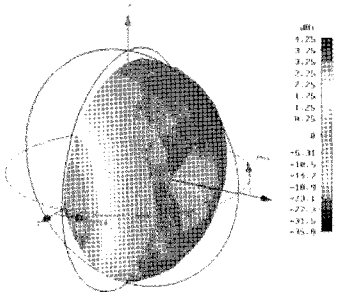

(c) Left polarization

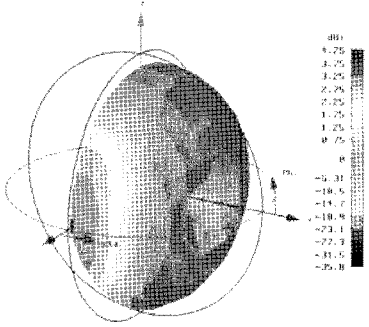

(d) Right polarization

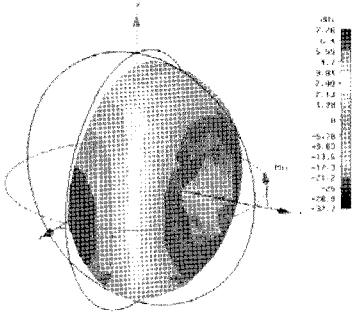

(e) Abs of far field radiation

5. Far-field radiation pattern of UWB antenna sensor in CST MS studio version 5.0

3. Experiment

3.1. Sensors Used in the Experiment

In the experiment, a commercial high frequency current transformer sensor is used as a reference sensor to confirm partial discharge signal compared with our newly designed UWB sensor. HFCT, an inductive coupling device sensing the induced ground current caused by PD, can detect the frequency range of 2 to 40MHz.

The above simulated UWB sensor is fabricated by a photolithographic etching process, making the construction relatively easy and inexpensive using PCB FR4 dielectric material.

A 50ΩSMA connector is connected to the microstrip feed line in sensor fabrication and the fabricated sensor picture and HFCT picture used in the test are shown in Fig. 6 (a) and (b), respectively.

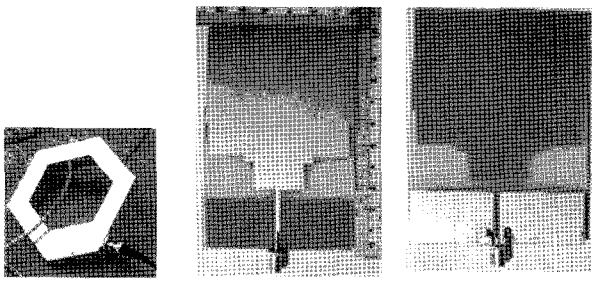

(a) (b)

Fig. 6. Picture of (a) HFCT sensor used in the Test and (b) fabricated UWB sensor

3.2. Experiment Setup

In the laboratory, a high voltage external source is used to energize the 22.9kV medium voltage XLPE cable and the sensors and measurement instruments are setup as shown in Fig. 7. The HFCT sensor is setup at the ground

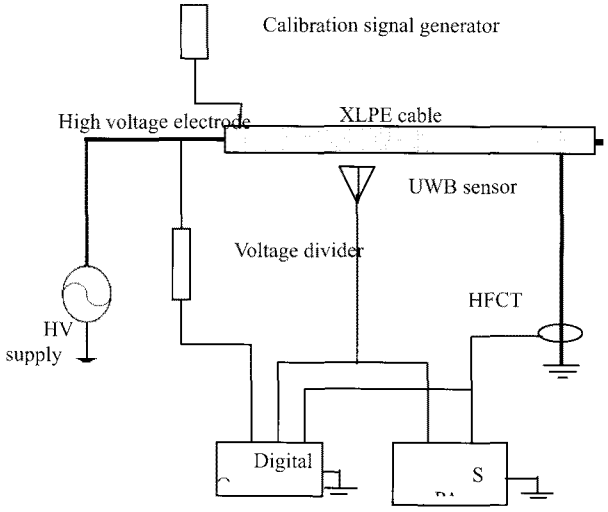

Fig. 7. Experimental setup in the laboratory

shield and its output and UWB sensor outputs are connected to a spectrum analyzer that gives the frequency domain results of the PD spectrum and connects to the digital oscilloscope to confirm the PD signal in time domain and phase resolve partial discharge pattern (PRPD) in high voltage cycle.

Before high voltage injection, a calibration signal generator, which can generate a signal of up to 100pC, is setup to the ground shield to inject the calibration signal to the cable.

A voltage divider is connected to the high voltage terminal to trigger a 50Hz AC waveform to confirm the discharge signal by PRPD pattern in the oscilloscope. Corona protection is setup at both sides of the cable end.

4. Test Results and Discussion

4.1. Time Domain Oscilloscope Results

The signal output results of both the commercial HFCT sensor and UWB sensor detection are checked by a digital oscilloscope to confirm the discharge signal with trigging 50 Hz Ac voltage. PD signal is always occurred at the region of positive rise time and negative rise time of applied voltage. According to the results shown in Fig. 8, the detected signals by both HFCT and UWB sensor are confirmed and the PD inception voltage of the 22.9kV XLPE cable is occurred at 19.5kV.

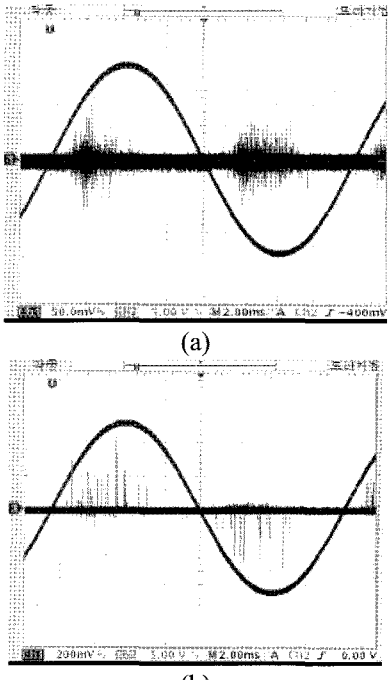

(a)

(b)

Fig. 8. Time domain oscilloscope results of (a) HFCT and (b) UWB sensor at 19.5kV injection

4.2. Frequency Domain Spectrum

The output of the UWB sensor is measured by spectrum analyzer to check the frequency spectrum of the detected signal. When 19.5 kV is applied to the cable, a partial discharge signal appears. First the frequency range of 0 to 100MHz is measured as revealed in Fig. 9 (a). Then frequency range is extended up to 1 GHz and PD signal can be occurred until 700 MHz as shown in Fig. 9 (b). Since this experiment is not set up in the external radio interference protected shield, we found that the UWB sensor received signals from the local radio stations around the frequency band of 100 MHz, 200 MHz, and 900 MHz.

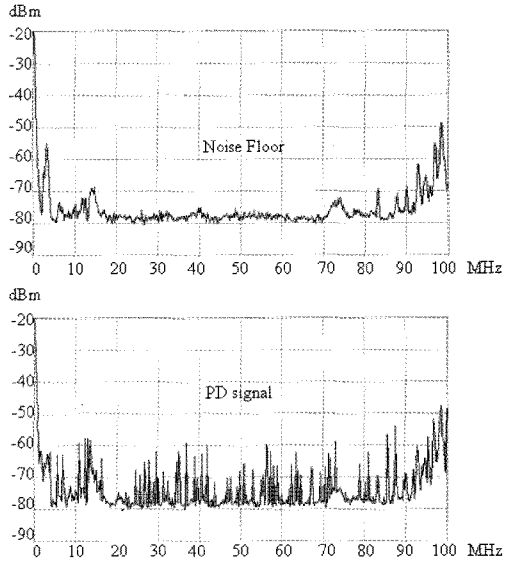

(a)

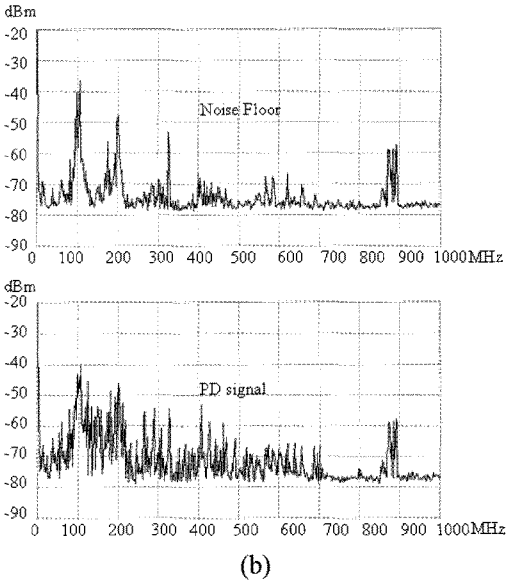

(b)

Fig. 9. Frequency domain discharge activity results of (a) 0 to 100MHz range (b) 0 to 1GHz range by UWB sensor when 19.5kV high voltage is injected.

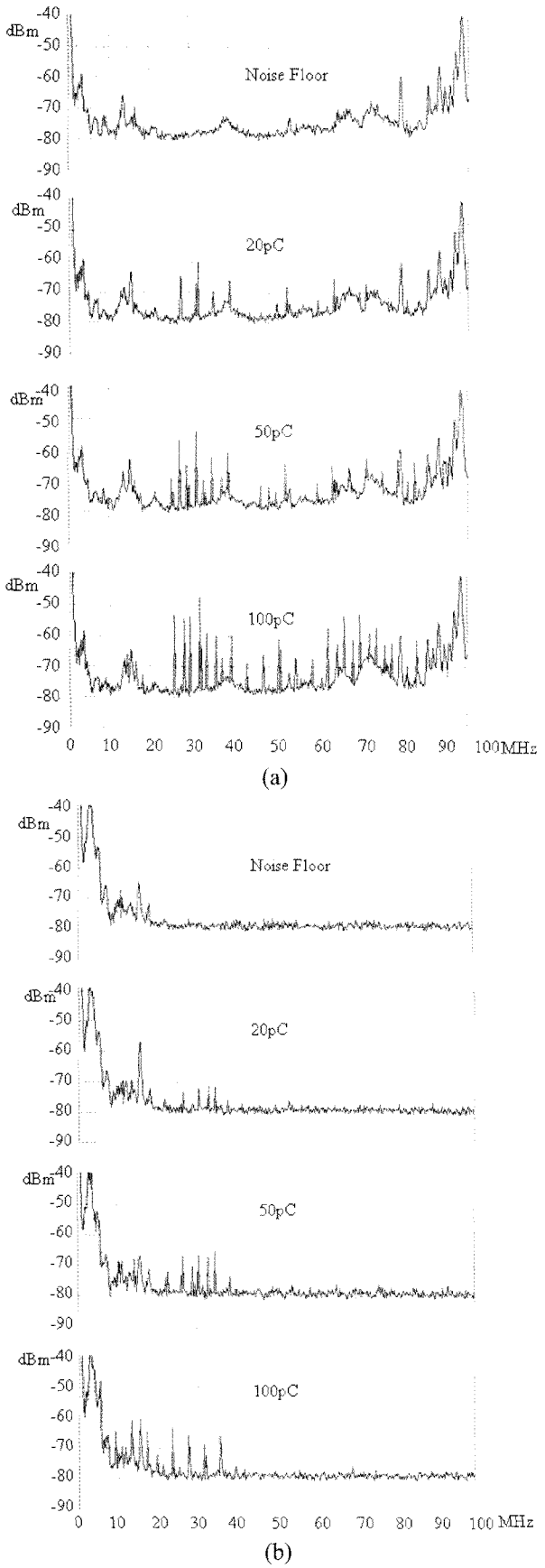

Fig. 10. Calibration signal spectrum detected by (a) UWB sensor and (b) HFCT sensor

But our UWB sensors can detect both lower frequencies and higher frequencies of PD signal and the peak value of the PD signal can be found around 400Mz with the amplitude of 53 dBm.

During calibration testing, the calibration signal generator injected 20pC, 50pC, and 100pC signals to the cable and the calibration signal spectrum is measured by both the HFCT and UWB sensors. The detected calibration spectrum of 20pC, 50pC, and 100pC are indicated in Fig. 10 (a) detected by UWB sensor and (b) by HFCT sensor.

The peak values of detected signals by HFCT and UWB sensors are compared as given in Fig. 11. It can be seen that the sensitivity of the UWB sensor is better than HFCT and that it can detect both low frequency signals and high frequency regions.

Moreover, the more discharge quantity, the higher the frequency spread. The comparison results of calibration

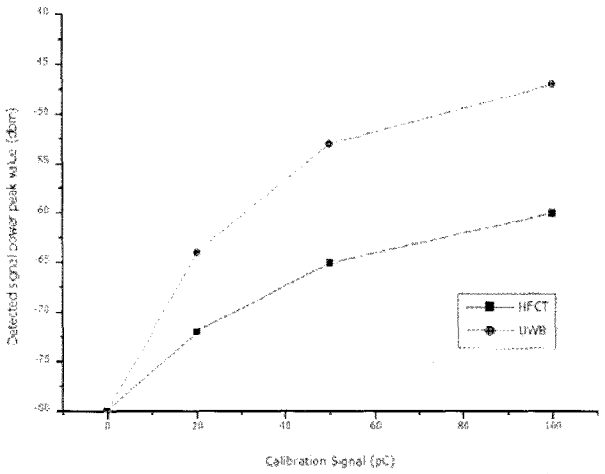

Fig. 11. PD signal peak value comparative results of HFCT and UWB sensor

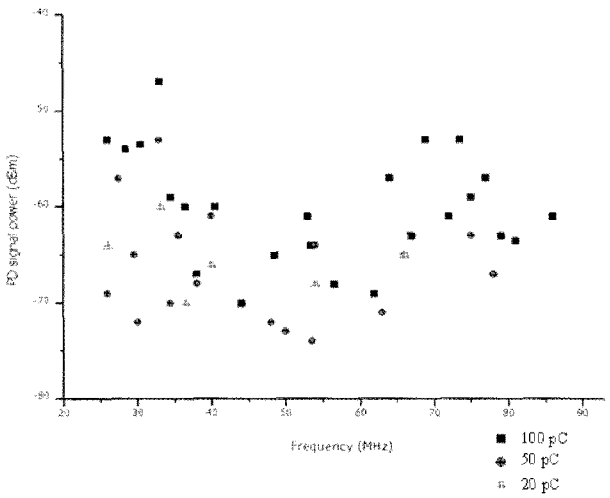

Fig. 12. The graph showing discharge activities spreading with different frequencies of different charge values detected by UWB sensor

signal spreading to higher frequency when the larger charge quantity is raised from 20pC to 100pC within 5s sweep time is shown in Fig. 12.

The maximum frequencies of 20pC, 50pC, and 100pC calibration signal are found at 66 MHz, 78MHz, and 86Mz respectively, and more electromagnetic pulses are spread out over different frequencies at larger charge quantity. Therefore, the ultra-wide band detection method is necessary to obtain the exact discharge signal energy or discharge quantity of both low frequency and high frequency bands.

5. Conclusions

As a conclusion, we verified that our new design of the low frequency compact UWB sensor can also detect partial discharge signals compared with the commercial HFCT sensor. Furthermore, the newly designed UWB sensor can detect a very wide range of signals of both low frequency and high frequency regions. According to the experiment results, by using the UWB sensor, greater discharge quantity and higher frequency were seen. Furthermore, the UWB sensor showed more sensitivity than the commercial HFCT sensor.

Moreover, our new UWB sensor is small in size *(110x64 mm^2)* and since it is fabricated on FR4 PCB, it is very lightweight compared with the conventional sensors such as HFCT, high voltage coupling capacitor, etc. As well, it is easy to integrate in the signal processing circuit and measuring system. It is also easy to fabricate and is cost effective. But if we use the UWB sensing technique in PD diagnosis, an external radio interference protected shield in the test room or noise cancellation circuit with external noise sensing antenna will be needed. Part of the future plan is to study the frequency domain of the discharge signal in detail and also to study the ultra-wide band PD signal and total signal energy or discharge quantity by using the UWB sensor.

Acknowledgement

This study has been sponsored by the Korea Electric Power Research Institute (R-2006-1-241-003) based on the support of the Electric Power Industry Technology Evaluation & Planning Department.

References

[1] R. Denissov, T. Grund, W. Klein, S. Tenbohlen, "UHF partial discharge diagnosis of plug-in cable terminations," Jicable, 2007.

[2] S. Gulski, A. R Samuel, L. Kehl, and H. T. F Geene, "Partial discharge location in HV cables with traveling system," *IEEE International Symposium on EI*, June 1996.

[3] N. H. Ahmed and N. N Srinivas, "Online partial discharge detection in cables," *IEEE trans. Diel. Elect. Insul.*, vol. 5, no. 2, pp. 181-188, 1998.

[4] N. de Kock, B Coric, and R. Pietsch, "UHF PD detection in GIS- suitability and sensitivity of the UHF method in comparison with the IEC 270 method," *IEEE Elect. Insul. Magazine*, vol. 12, no. 6, pp. 20-26, 1996.

[5] M. Kawada, "Ultra wide-band UHF/VHF ratio interfereometer system for detecting partial discharge source," *IEEE Trans*, 2002.

[6] D. M Pozar and D. H. Schaubert, "Microstrip antenna: the analysis and design of microstrip antennas and arrays," *IEEE Express*, 1995.

[7] R. Garg, P. Bhartia, I. Bahl, and A. Ittipiboon, *Microstrip Antenna Design Handbook*, Artech House, 2000.

[8] J. Jung, "A small wide-band microstrip-fed monopole antenna," *Microwave Opt Technol Lett 15*, 2005.

[9] J. Kim, "Design of an ultra wide-band printed monopole antenna using FDTD and genetic algorithm," *IEEE microwave Wireless Compon Lett 12*, 2002.

[10] S.-W. Su, K.-L. Wong, and C.-L. Tang, "Ultra-wide-band square planar monopole antenna for IEEE 802.16a operation in the 2-11GHz band," *Micriowave Opt Technol Lett 42*, 2004.Trans, 2002.

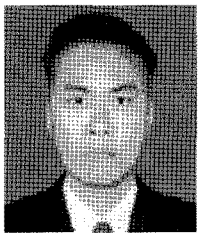

Kyaw Soe Lwin

He received his B.E degree in Electronic Engineering from Mandalay Technological University, Myanmar, in 2001 and his M.E (electronic) degree from Yangon Technological University, Myanmar, in 2005. He is currently studying for his Master's Course at the Department of Electrical, Electronic & Information Eng. at Wonkwang University, Korea. His research interests include EM sensing and diagnosis in high voltage insulation.

Kwang-Jin Lim

He graduated from the Division of Electrical Electronic Engineering at Wonkwang University in 2007. He is currently taking a Master's Course in the Department of Electrical Materials, Wonkwang University. His main research interests are insulation, high voltage discharge, and partial discharge diagnosis in HV insulation.

Noh-Joon Park

He received his B.S., M.S., and Ph.D. degrees in Electronics Engineering from Wonkwang University in 1993, 1995, and 2004, respectively.

Since 2006, he has been a Research Professor with the Center for Advanced Electric Applications at Wonkwang University working on the design and analysis of EM sensors for partial discharge diagnosis in high voltage engineering and electronic circuit design with impedance matching technique for light sources.

Dae-Hee Park

He was born in 1954 in Korea. He received his B.S. and M.S. degrees in Electrical Engineering from Hanyang University in 1979 and 1983, respectively, and his Ph.D. degree from Osaka University in 1989. He worked at the LG Cable Research Institute as a Senior Researcher from 1979 to 1991. After that, he joined the School of Electrical, Electronics and Information Engineering at Wonkwang University where he is currently employed as a Professor. He has also worked as Director of the "Center for Advanced Electric Application" from 2004 at Wonkwang University. He was at MSU in the USA as a Visiting Professor from 1999 to 2000. His main research interests are in the areas of insulting and dielectric materials, new lighting sources, and discharge. He is a member of the Korean IEE, Korean IEEME, and IEE Japan.